Universidade do Minho
Escola de Engenharia

IMS
International Masonry Society

9ᵗʰ International Masonry Conference 2014 in Guimarães

NUMERICAL MODELLING OF MASONRY-INFILLED REINFORCED CONCRETE FRAMES: MODEL CALIBRATION AND PARAMETRIC STUDY

Farhad Akhoundi[1], Paulo B. Lourenço[2], G. Vasconcelos[3]

ABSTRACT: Generally two methods are proposed for analyzing the infilled frames; Micro modelling approach which finite element method is used to take into account local effects in detail and Macro modelling approach which is a very simplified method that takes into account the global behavior of the structure by replacing the infill with diagonal strut.

In the present study a numerical analysis is carried out on a one bay one storey reinforced concrete frame with masonry infill under in-plane loading by using finite element modelling through the DIANA software. The numerical model was calibrated based on experimental results and then a parametric study was carried out, taking into account variation of material properties of infill and its height to length ratio. It is concluded that compressive strength and height to length ratio of the masonry infill has dominant role on the in-plane behavior of these types of masonry infilled frames. Increasing the compressive strength of the masonry enhances the lateral strength of the infilled frames while increasing the height to length ratio of the infill panel results in decrease of their lateral strength and initial stiffness.

Keywords: masonry-infilled reinforced concrete frame, in-plane loading, micro modelling approach, DIANA software

1. INTRODUCTION

Last seismic events in Southern Europe have highlighted the vulnerability in the most usual constructive typology in contemporary architecture: framed structures with masonry infills [1]. Contemporary structures have a good capacity to withstand these actions, given that they were considered for their design according to modern codes. Nonetheless, nonstructural elements as masonry infills show a high degree of damage even for medium magnitude earthquakes, causing casualties and high economic losses [2, 3]. For decades, these elements have been considered as nonstructural and therefore they were not requested to have resisting conditions.

Several experimental studies have been carried out to investigate the effect of masonry infills on the in-plane behavior of masonry infilled frames. Some of them were concentrated on reinforced concrete frames [2, 4-6] and some on steel frames [7, 8]. Although masonry infills are assumed as non-structural elements, their presence can affect the global behavior of the infilled frames by increasing its stiffness, lateral strength and energy dissipation capacity [4, 7] or causing the failure of

[1] Ph.D candidate, ISISE, Civil Engineering department, Minho University, farhad.akhoundi@civil.uminho.pt
[2] Professor, ISISE, Civil Engineering department, Minho University, pbl@civil.uminho.pt
[3] Professor, ISISE, Civil Engineering department, Minho University, graca@civil.uminho.pt

the system by forming short column effect or soft story phenomenon [9]. Mehrabi et al [4] concluded that the lateral strength of the reinforced concrete frame with masonry infill is 175% higher than that of a bare frame. In the another study carried out by Yuksel et al [10], it was concluded that the presence of infills increases the lateral strength of the bare frame about 100%. These conclusions highlight the importance of the infills within frames to be considered in the design process of the buildings.

Experimental results confirm that there are important parameters which could affect the in-plane behavior of infilled frames [11, 12]. Those parameters could be classified in three different categories; (a) geometry and mechanical properties of the infill; (b) geometry and mechanical properties of the surrounding frame; (c) condition of the infill-frame interface. In the study carried out by Kakaletsis et al [12] it was concluded that the specimens with strong infills demonstrate better performance than those with weak infills in terms of lateral strength, stiffness, ductility and energy dissipation capacity. Several studies were concentrated on the effect of opening and its position on the in-plane behavior of the infilled frames [8, 12] and a detailed state-of-the-art was conducted by Surendran et al [13]. The characteristics of the interface between masonry infill and its surrounding frame can also affect the infilled frame's behavior [11, 14]. The unintentional gap between the infill and surrounding frame, which is generally the result of masonry shrinkage is one of those parameters and unless this gap is not closed, the masonry infill will not contribute to the lateral in-plane behavior of the structure. Using shear connectors along the whole perimeter of the interface enhances the behavior of the structure by increasing its lateral strength and stiffness [14].

Numerical analysis provides better insight into understanding the exact behavior of the infilled frames. This needs a validated numerical model which is calibrated by experimental results. In this paper it is intended to numerically investigate how the variation in mechanical properties of masonry infill and also its geometry affect the in-plane behavior of infilled frames.

Generally there are two methods for numerically analyzing the infilled frames, namely macro and micro modelling approaches. In the Macro modelling approach, infill is replaced by equivalent diagonal strut [15]. Experimental results revealed that the equivalent strut must have a width to accurately represent the infill. Different studies were carried out to determine the width of the diagonal strut [16, 17]. The single diagonal strut method is a simple and capable of representing the global behavior of the infill but it cannot predict local effects in the infill resulting from interaction between infill and frame. To overcome this, different strut models such as double-strut, triple-strut with different configurations have been proposed [18, 19].

In the micro modelling approach finite element method is used to model the infill panel which contributes to better understanding of the local behavior of the infilled frames. As it is shown in **Erro! A origem da referência não foi encontrada.**Figure 1 there are three different approaches to model the infill in micro modelling approach, namely detailed micro model, simplified micro model and macro model by considering a masonry as homogenous and isotropic material (which is totally different with macro model that infill is replaced by diagonal strut) [20]. In the detailed micro modelling approach infill panel is modelled as a set of three different components: brick, mortar and interface between mortar and brick. In the simplified micro model, infill is modelled as a set of two different elements: expanded brick and interface elements. Interface elements represent the behavior of the mortar and also the interface between mortar and brick.
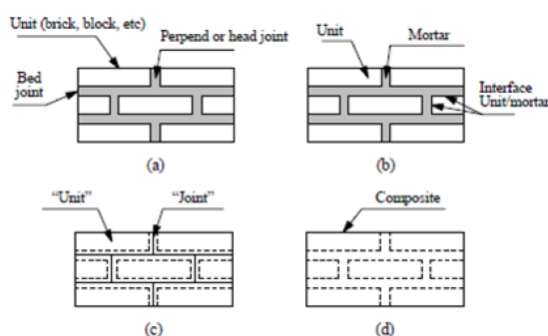
Figure 1 Various techniques in micro modelling approach: (a) part of a masonry wall; (b) detailed micro-model; (c) simplified micro-model; (d) macro-model

2. NUMERICAL MODELLING

To fulfil the objectives of this study and carry out a parametric study by evaluating some factor in the in-plane behaviour of brick masonry infilled RC frames, a calibration of a finite element model was previously carried out. The calibration of the numerical model in DIANA software was made based on the experimental results obtained by Pereira [5] on the in-plane static cyclic tests on masonry infilled RC frames. In the experimental program three different test specimens were considered and its description in terms of materials and geometry is presented in Table 1Table 1. The mechanical properties are represented in Table 2Table 2 and a general overview of the reinforcing scheme and geometry of the RC frame are represented in Figure 2Figure 2.
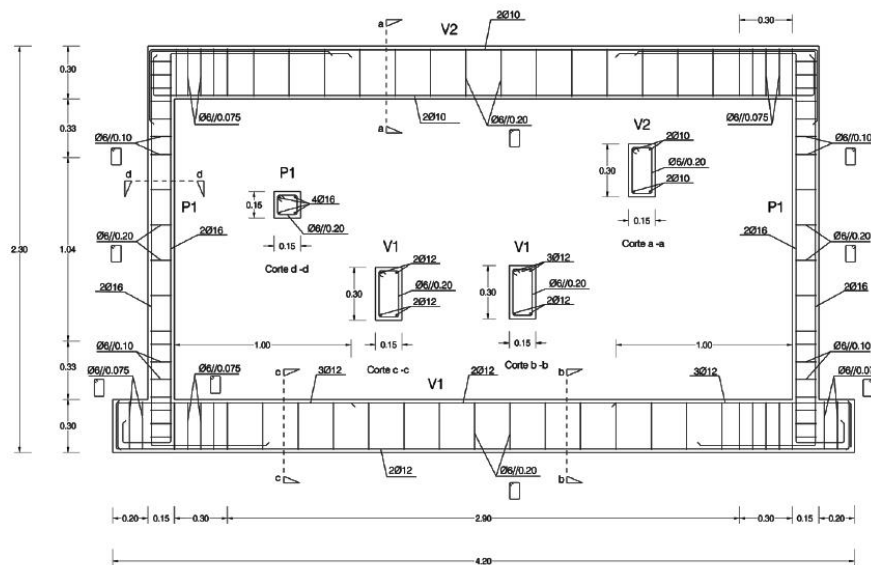

Figure 2 Geometry and reinforcement scheme of the specimens

Table 1 Properties of test specimens

Specimen	Type of Panel	Components	Characteristics
Wall-Ref-01	Simple (without rendering)	Brick Mortar	With dimensions of 30*20*15 cm Mortar M5 with 1 cm thickness
Wall-Ref-02	Simple (with rendering at both sides)	Brick Mortar Rendering	With dimensions of 30*20*15 cm Mortar M5 with 1 cm thickness Mortar M5 with 1 cm thickness at each sides
Wall-JAR	Reinforced panel	Brick Mortar Exterior rendering Interior rendering Reinforcement	With dimensions of 30*20*15 cm Mortar M5 with 1 cm thickness Mortar M5 with1 cm thickness Projected Gypsum 2ϕ4 at bed joints

Table 2 Mechanical properties of the infilled frame's components

Mechanical Properties	Concrete	Masonry	Reinforcement
Elastic Modulus perpendicular to the bed joints (GPa)	31.5	1.6715	200
Poisson's ratio	0.15	0.13	-
Tensile Strength (MPa)	2.35	0.25	-
Mode-I Tensile Fracture Energy (N/mm)	0.1	0.017	-
Compressive Strength (MPa)	31.5	1	-
Compressive Fracture Energy (N/mm)	8	1	-

Yield Stress (MPa)	-	-	400

The numerical model of the specimens was defined by using micro modelling approach but considering the infill panel as a homogenous material as described before. Masonry infill and concrete frame was modelled by using four-noded shell elements. Reinforcement was added to the concrete frame by embedding them to the concrete elements. Interface elements of (2+2) noded were used to model the behavior of the interface between masonry infill and reinforced concrete frame. The mesh of the finite element model of the test specimen is shown in
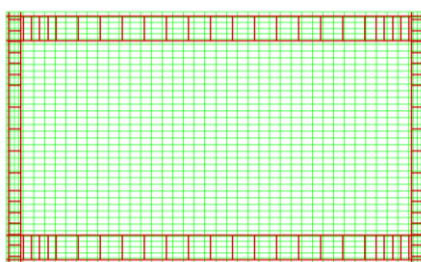
Figure 3Figure 3.

Figure 3 Finite element model of the test specimen

A constitutive model of "total strain fixed crack" based on total strain which can describe the tensile and compressive behavior of the material with one stress-strain relationship was used for modelling masonry and concrete materials. Furthermore multi surface interface model of "combined cracking-shearing-crushing" as shown in Figure 4Figure 4 is used to simulate fracture, frictional slip as well as crushing along the interface.
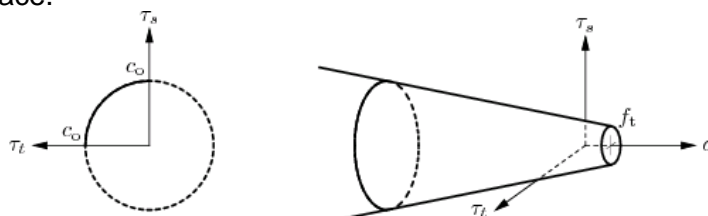

Figure 4 Three-dimensional interface yield function

Vertical load of 50KN was applied to the columns in the numerical model in accordance to what was considered in the experimental program to simulate the weight of the upper storeys. Three translations and three rotations of bottom beam and also out-of-plane translations of the upper beam were fixed to simulate the constraints of the RC frame in a similar manner to what made in the experimental tests.

Mechanical properties of the interface between masonry infill and its surrounding frame represented in Table 3Table 3 were obtained by validating the numerical force-displacement diagram of Wall-Ref-01 in comparison to the experimental diagram obtained in the static cyclic tests along with its crack patterns with test results.

Table 3 Mechanical properties of the interface elements

Elastic Properties		Nonlinear Properties		
Normal stiffness (N/mm^3)	Shear Stiffness (N/mm^3)	Tensile Strength (MPa)	Mode I fracture Energy (N/mm)	Cohesion (MPa)
9.26	5.447	0.05	0.05	0.07
Nonlinear Properties				

Tangent of Friction Angle	Dilatancy	Mode II fracture energy (N/mm)	Compressive Strength (MPa)	Compressive fracture energy (N/mm)
0.5	0.0001	0.3	30	8

As it is shown in Figure 5Figure 5a the force-displacement diagram of the validated numerical model of Wall-Ref-01 is almost an average of the test results. This confirms that numerical model is close to test results. Because the tests were performed cyclically, "Test+" represents the monotonic envelop diagram of the specimen in –x direction and "Test-" represents the monotonic envelop diagram in +x direction.

At low lateral load levels applied to the infilled frame, masonry infill and its surrounding frame act as monolithic load resisting system but by increasing the lateral load masonry infill separates from its bounding frame and forms diagonal strut as shown in Figure 5Figure 5b to withstand the applied load. Right after separating the masonry from RC frame in left upper corner at lateral load of 55KN, it separates in right bottom corner at lateral force of 65KN which is similar to what happened in test specimens.
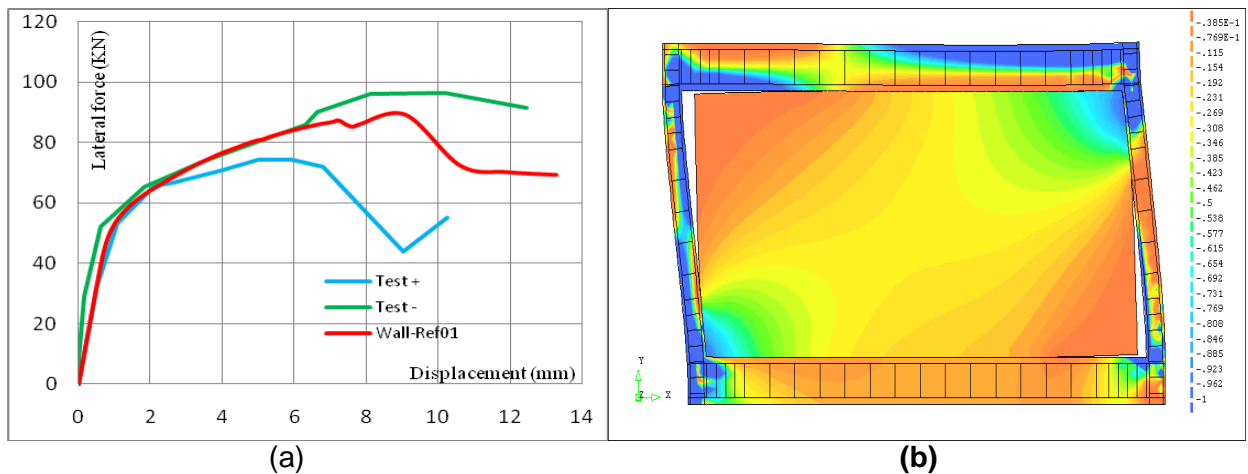

(a) (b)

Figure 5 a) comparison of the numerical force-displacement diagrams with the monotonic experimental envelop obtained in both loading directions b) distribution of principal minimum stress within infilled frame

Deformed mesh of the infill panel in the numerical model which is shown in Figure 6Figure 6a indicates that the masonry infill crushes in both corners at the diagonal compression strut. This crushing of the both ends is also observed in experimental results as is shown in Figure 6Figure 6b.

Aiming at evaluating the performance of the validated model based on the specimen Wall-Ref-01, it was important to assess the ability of the validated model for predicting the experimental behavior of the test specimens of "Wall-Ref-02" and "Wall-JAR". To do this, Numerical models of Wall-Ref-02 and Wall-JAR were made by using their infill's mechanical properties as represented in Table 4Table 4 and modifying the interface mechanical properties of Wall-Ref-01 since presence of rendering will change its properties. For instance the tensile strength of the interface for Wall-Ref-02 and wall-JAR was calculated by taking into account the tensile strength of layers of rendering as;

$$f_{tin} = \frac{(f_{ti} \times t_w) + (f_{tr} \times t_r)}{t_{all}}$$
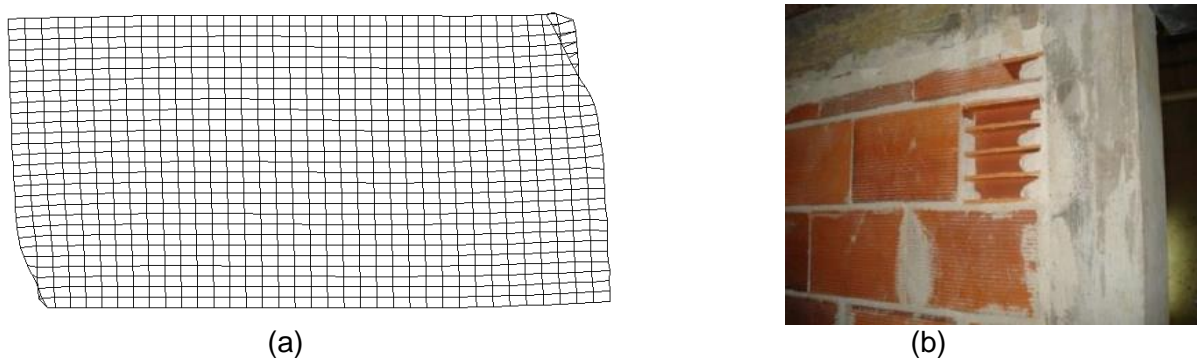
Eq. 1

| (a) | (b) |

Figure 6 Details of the calibration of the numerical model; (a) Deformed mesh of the infill in numerical model; (b) crushing the loaded corner in the test specimen

In which f_{tin} is the tensile strength of the interface in new condition (after adding rendering), f_{ti} is the tensile strength of the interface before adding the rendering, f_{tr} is the tensile strength of the added materials, t_w is the thickness of the infill wall before adding the rendering (15 cm), t_r is the thickness of the added materials (1 cm) and t_{all} is the all thickness of the wall after rendering.

Mechanical properties of the interface in shear such as cohesion, Mode I and Mode II fracture energies were calculated in the same way by replacing the tensile strength with cohesion, Model and Mode II fracture energies in Eq. 1~~Eq. 1~~ respectively as represented in Eq. 2~~Eq. 2~~ to Eq. 4~~Eq. 4~~. Calculated mechanical properties of Interface for Wall-Ref-02 and Wall-JAR are represented in Table 5. Because the compressive mechanical properties of the interface for Wall-Ref-01 are high enough, they did not recalculated for interfaces with rendering.

$$C_{in} = \frac{(C_i \times t_w) + (C_r \times t_r)}{t_{all}}$$ Eq. 2

$$M_{in}^I = \frac{(M_i^I \times t_w) + (M_r^I \times t_r)}{t_{all}}$$ Eq. 3

$$M_{in}^{II} = \frac{(M_i^{II} \times t_w) + (M_r^{II} \times t_r)}{t_{all}}$$ Eq. 4

In which C_{in}, M_{in}^I and M_{in}^{II} are the cohesion, Mode I fracture energy and Mode II fracture energy of the interface in new condition respectively, C_i, M_i^I and M_i^{II} are the chesion, Mode I fracture energy and Mode II fracture energy of the interface before adding the rendering respectively and finally C_r, M_r^I and M_r^{II} are the cohesion , Mode I fracture energy and Mode II fracture energy of the rendering materials respectively.

Table 4 Mechanical properties of infill used for modelling Wall-Ref-01 and Wall-JAR

Mechanical Properties	Infill Wall-JAR	Infill Wall-Ref-02
Young Modulus (GPa)	4.43	3.83
Poisson's ratio	0.175	0.237
Tensile Strength (MPa)	0.5	0.4
Mode-I Tensile Fracture Energy (N/mm)	0.03	0.03
Compressive Strength (MPa)	1.97	1.26
Compressive Fracture Energy (N/mm)	1	1

Table 5 Mechanical properties of interface after rendering

Interface mechanical Properties	Wall-Ref-02	Wall-JAR
Tensile strength (MPa)	0.13	0.18
Mode I fracture energy (N/mm)	0.13	0.18
Cohesion (MPa)	0.2	0.263
Mode II fracture energy (N/mm)	0.9	1.1

According to what is seen from Figure 7Figure 7, static nonlinear analysis of the numerical force-displacement diagrams of Wall-Ref-02 and Wall-Jar shows that they satisfactorily can represent the experimental results of these wall specimens.
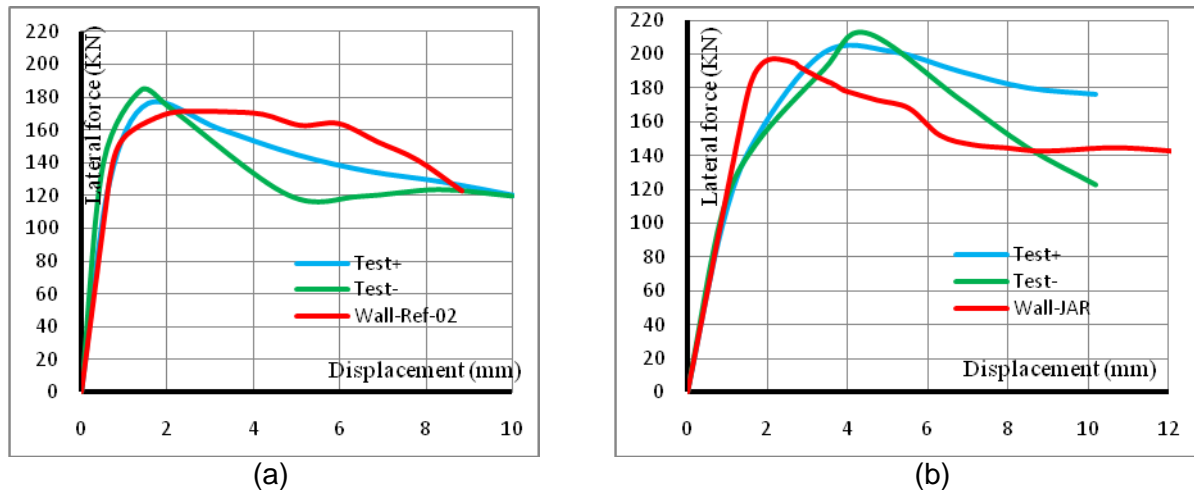

(a)   (b)

Figure 7 Comparison between numerical and experimental force-displacement diagrams; (a) Wall-Ref-02; (b) Wall-JAR

3. PARAMETRIC ANALYSIS

After the calibration of the numerical model, it was decided to make a parametric analysis to evaluate the influence of the mechanical properties of the masonry infill such as compressive strength, compressive fracture energy, tensile strength and elastic modulus on the global response of the infilled frames under in-plane loads. Besides the material properties of the brick masonry, also the geometric properties, namely the height to length aspect ratio was also taken into account.

3.1. Effect of Infill's compressive strength

In a first numerical analysis, the compressive strength of brick masonry was taken as 2MPa and 5MPa to investigate the effect of its variation on the in-plane behavior of infilled frames. As it is shown in Figure 8Figure 8 increasing the infill's compressive strength leads to increase in the lateral strength of the infilled frame.

By increasing infill's compressive strength from 1MPa (used in the calibration of the numerical model) to 2MPa, infilled frame's lateral strength increased about 15% while by increasing its compressive strength from 2MPa to 5MPa, the increase in its lateral strength is 64%. The improvement of the lateral strength of the masonry infilled RC frame by increasing the compressive strength of masonry is much associated to the crack patterns and damage developed in the composite structure. In fact, the damage pattern is much related to the crushing of masonry at the ends of the compression strut at the contact between the masonry infill and the frame. This means that by increasing the compressive strength of masonry, the damage due to masonry crushing is delayed and occurs for higher values of stresses developed in the walls, corresponding to higher values of the lateral load applied.
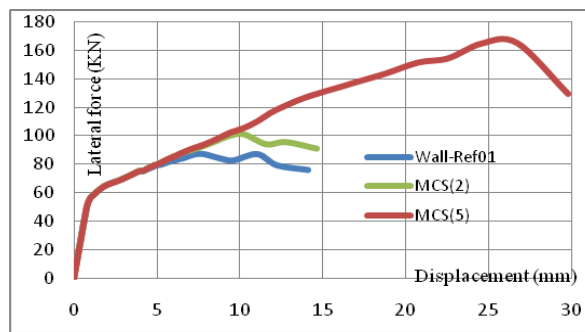
Figure 8 Pushover diagrams of the numerical models

Usually the masonry materials with higher compressive strengths have higher fracture energies. To simulate this condition, infill's compressive strength and also its compressive fracture energy in Wall-Ref-01 was increased for two times to have the compressive strength of 2MPa and compressive fracture energy of 2N/mm. The results of static nonlinear analysis in term of force-displacement diagrams are shown in Figure 9~~Figure 9~~.
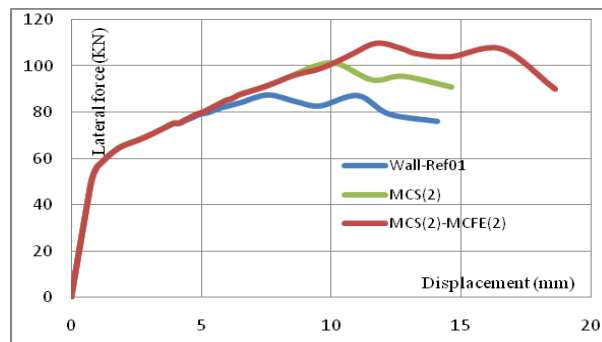

Figure 9 Pushover diagrams of the numerical models

It can be concluded that increasing the infill's compressive strength from 1MPa to 2MPa and also its compressive fracture energy from 1N/mm to 2N/mm together cause increase of the maximum lateral strength about 23%. Comparing the force-displacement diagrams of the MCS(2) and MCS(2)-MCFE(2) demonstrates also that by increasing the compressive fracture energy higher non-linear displacement capacity of the composite structure is achieved leading also to the smoothing of the post peak behavior of the structure, see the post peak branch of wall specimen of MCS(2)-MCFE(2).

3.2. Effect of Infill's tensile strength

The effect of the tensile strength of brick masonry infill wall on its in-plane behavior and lateral resistance is evaluated by varying the tensile strength of masonry from 0.25MPa in the previously calibrated numerical model (Wall-Ref-01) to 0.5MPa. The tensile fracture energies are kept constant to investigate only the effect of tensile strength on the in-plane behavior. From the results obtained, it is observed that force-displacement diagram of the model with increased tensile strength do not show any change in terms of maximum lateral strength, see Figure 10~~Figure 9~~. Load-displacement diagrams of both models are the same until the peak load, which means that infill's tensile strength does not have significant effect on the load-displacement diagrams of these types of infilled-frames until the peak loads. Beyond the peak load, not significant minor changes were also recorded.
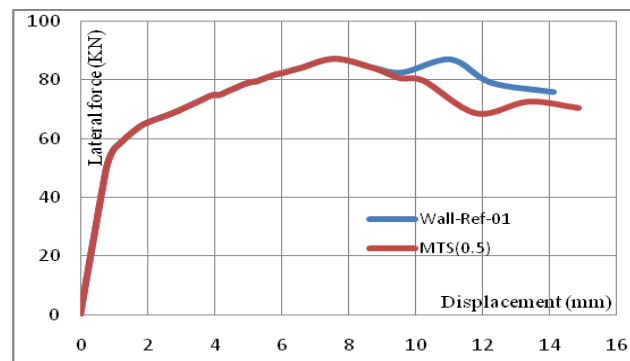
Figure 10 Comparison of the force-displacement diagrams for models with varying tensile strength of masonry

3.3. Effect of Infill's elastic modulus

The effect of the elastic stiffness of the masonry infill in the in-plane behavior of the masonry infilled RC frames is analyzed by increasing its elastic modulus about 100%. As it is shown in Figure 11Figure 11, 100% increasing the elastic modulus of the infill panel increases the initial stiffness of the infilled frame about 80% and its lateral strength about 5%, which appears to be negligible. The first crack in reference infill panel develops at a displacement of 9.6mm, whereas in the wall with increased elastic modulus the first crack develops at lateral displacement of 2.8mm. This means that in the panel with increased elastic modulus the cracking develops earlier with respect to reference wall. The great difference in the response of the composite structure to in-plane lateral loading is the deformation corresponding to maximum lateral load and also the maximum lateral displacement of the infilled RC frame. This appears to indicate that the use of less stiff infill masonry leads to considerably more ductile behavior of RC infilled frames.
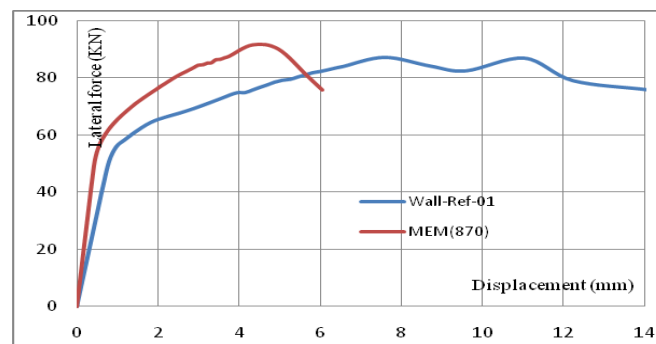

Figure 11 Force-displacement diagrams for RC frame models with distinct stiffness of the brick masonry infill

3.4. Effect of height to length ratio of the panel

In this section it is intended to investigate the effect of height to length ratio of the infill panel on the in-plane behavior of infilled frames. To do this, three walls with different lengths of 100, 200 and 500cm with height to length ratios of 1.7, 0.85 and 0.34 were assumed to be analyzed and compared with the analysis results of reference wall of Wall-Ref-01 that has a length of 350cm and height to length ratio of 0.47. The geometry of the specimens is represented in **Figure 12**Figure 12. The main reason to have different height to length rations by changing the infill's length is that in one specific storey within building that has a constant height, walls with different lengths can often be found.
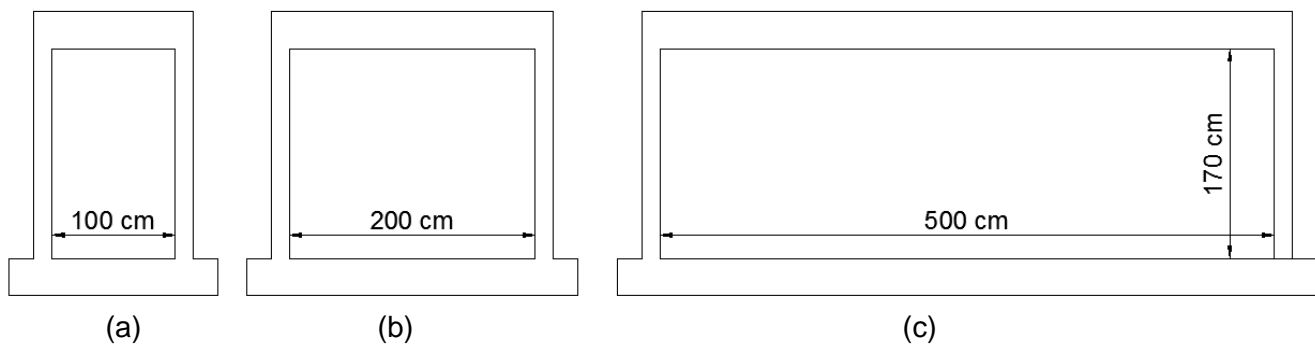
| (a) | (b) | (c) |

Figure 12 Geometrical configurations of the masonry infilled frames; a) h/l(1.7) b) h/l(0.85) c) h/l(0.34)

Static nonlinear analysis was carried out on the distinct walls to investigate their behavior under lateral in-plane loading. Force-displacement diagram of the all numerical models are represented in Figure 13Figure 13. By comparing the force-displacement diagrams of the numerical models it can be observed that by increasing the length of the reference model of Wall-Ref-01 from 350cm to 500cm which leads to a decrease of the h/l ratio from 0.47 to 0.34, model represents higher lateral strength and also higher initial stiffness. Initial stiffness is defined as tangent of line connecting the first point in graphs to the point corresponding to 30% of maximum lateral force. From the values of the lateral strength and initial stiffness of the numerical models presented in Table 6Table 6 it can be seen that the increase of the h/l ratio from 1.7 to 0.34 result in a reduction on lateral strength of about 46% and a reduction on the lateral stiffness of about 75%. Decreasing the length of the reference numerical model from 350cm to 200cm leads to decrease in the initial stiffness and lateral strength about 38% and 7% respectively.
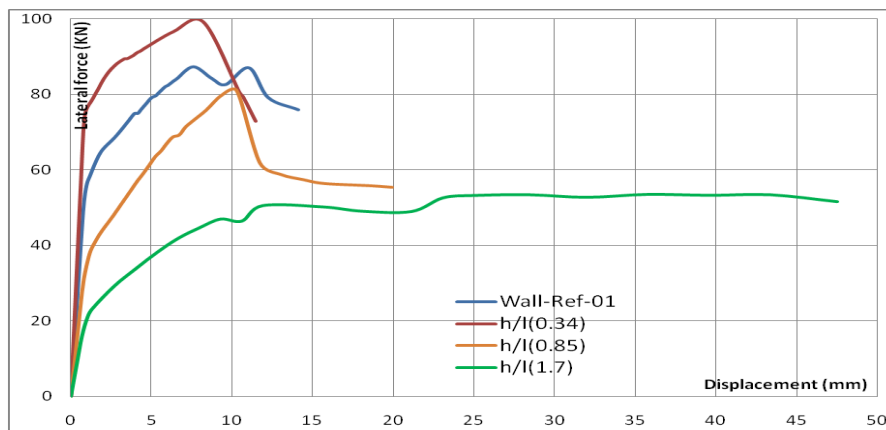

Figure 13 Forcee-displacement diagrams of the numerical models with different height to length ratios

In numerical models with h/l ratios less than 0.85, the force-displacement diagram presents a sudden drop. For higher values of the h/l ratio the behavior is considerably more ductile, such in case of the numerical model with h/l of 1.7. In the other words, numerical models with h/l ratios of less than 0.85 show brittle behavior while the numerical model with higher h/l ratio (1.7) shows very ductile behavior.

Table 6 Initial stiffness and lateral strength of the numerical models

Numerical Model	h/l	Initial Stiffness (N/mm)	Lateral Strength (N)
h/l(0.34)	0.34	91940	99100
Wall-Ref-01	0.47	65310	87250
h/l(0.85)	0.85	40110	80870
h/l(1.7)	1.7	23340	53480

The distribution of the minimum principal stresses for distinct masonry walls along with their general deformations for a lateral load of 40KN is represented in Figure 14Figure 14. As concluded before, higher h/l ratios leads to lower initial stiffness and thus to higher deformations. The same lateral load causes more deformations in the model h/l(1.7). In this model the infill panel is totally separated from its bounding frame and diagonal strut is completely formed under the lateral force of 40KN. In both ends of diagonal strut the compressive stresses surpasses the compressive strength of masonry. By increasing the length of the infill, h/l(0.85), a small amount of separation happens under the same lateral load. The diagonal strut has formed but the compressive stresses in its both ends are lower than the compressive strength and thus can withstand more lateral loads. In the numerical model h/l(0.34), the separation has not been occurred under lateral load of 40KN and it must be increased to even separate its infill from the RC frame. In this condition the infill and its surrounding frame monolithically resist the lateral load. It is clear that this numerical model withstand more lateral load as represented in Table 6Table 6.

Crack patterns of the numerical models of h/l(1.7), h/l(0.85) and Wall-Ref-01 along with their deformations under lateral load are represented in Figure 15Figure 15. Because the crack pattern of both models of Wall-Ref-01 and h/l(0.34) is similar, the crack pattern of Wall-Ref-01 is represented. The magnification factor for all the numerical models in Figure 15Figure 15 are the same. In the crack pattern developed in the Wall-Ref-01, the masonry crushes in both ends of the diagonal strut and cracks in vicinity of the right column by formation of some minor tensile cracks.
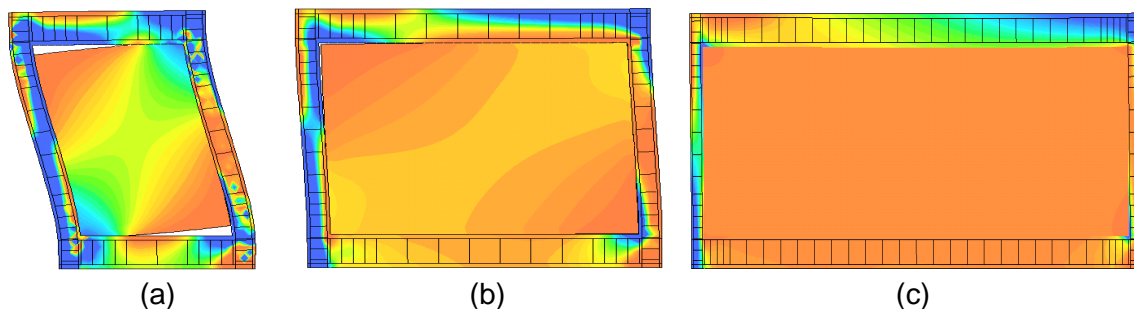

(a)   (b)   (c)

Figure 14 Distribution of the minimum principle stresses within the frame under lateral force of 40KN: a) h/l(1.7) b) h/l(0.85) c) h/l(0.34)

By moving from numerical model of Wall-Ref-01 to h/l(0.85), it can be observed that although the masonry crushes in both ends of the strut but some tensile cracks form which connects the crushed corner to the opposite corners in a horizontal direction. Formation of horizontal cracks in bottom part of the infill could be interpreted as the effect of increasing height to length ratio resulting in higher in-plane flexural stresses.

In the numerical model of h/l(1.7), the separation of the infill from its bounding frame is large enough with respect to the other numerical models which is due to higher h/l ratio. This could be assumed as the main reason for formation of extensive horizontal cracks in bottom part of the infill.
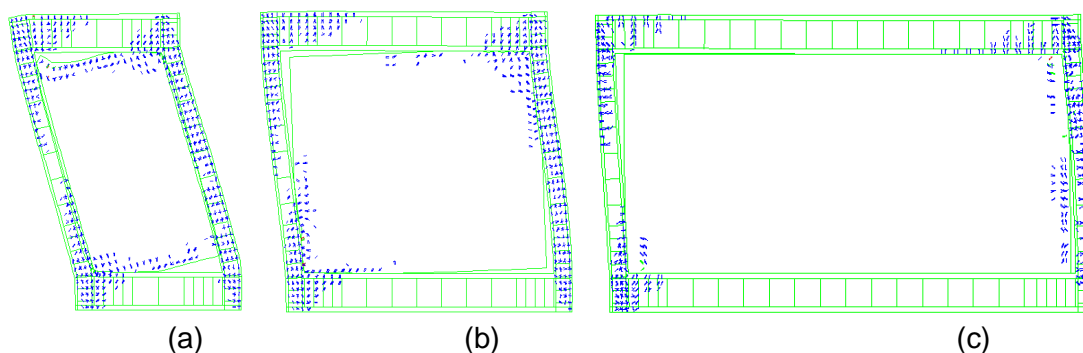

(a)   (b)   (c)

Figure 15 Crack patterns of the infilled frames of a) h/l(1.7) b) h/l(0.85) c)Wall-Ref-01

4. Conclusions

A parametric analysis is presented in this paper in order to investigate the influence of variation in mechanical properties of the infill and also its geometry on the in-plane behavior of masonry infilled frames. The following conclusions can be drawn from the present study:

1. Compressive strength of the masonry infill has dominant role in the in-plane behavior of masonry infilled frames. Presence of strong masonry in terms of compressive strength enhances the lateral strength of the infilled frame.
2. Increasing tensile strength of the infill panel does not appear to enhance the lateral strength of the infilled frame.
3. Increasing the elastic modulus of masonry infill increases the initial stiffness of the infilled frame but no changes on the lateral strength were achieved. The great influence of the elastic modulus of the masonry infill is in the in the increasing the brittleness of the composite structure. The deformation at peak load reduces significantly and almost post peak response is recorded.
4. Increasing h/l ratio of the infill decreases the initial stiffness and lateral strength of the infilled frame. For instance increasing the h/l of the infill from 0.34 to 1.7 decreases the initial stiffness and lateral strength of the infilled frame about 75% and 45% respectively.
5. Increasing the h/l ratio of the infill changes the crack pattern of the infilled frames.

ACKNOWLEDGEMENTS

REFERENCES

[1] Lourenço PB, Vasconcelos G, Medeiros P, Gouveia J. Vertically perforated clay brick masonry for loadbearing and non-loadbearing masonry walls. Construction and Building Materials. 2010;24:2317-30.
[2] Bertero V, Brokken S. Infills in seismic resistant building. Journal of Structural Engineering (ASCE). 1983;109:1337–61.
[3] Al-Chaar G, Issa M, Sweeney S. Behavior of Masonry-Infilled Nonductile Reinforced Concrete Frames. Journal of Structural Engineering. 2002;128:1055-63.
[4] Mehrabi AB, Shing PB. Performance of Masonry-Infilled R/C Frames under In-Plane Lateral Loads: Analytical Modelling. Proceedings from the NCEER Workshop on Seismic Response of Masonry. San Francisco, California1994. p. 45-50.
[5] Pereira MFP. Avaliação do desempenho das envolventes dos edifícios face à acção dos sismos: Universidade do Minho; 2013.
[6] Kyriakides MA. Seismec Retrofit of Unreinforced Masonry Infills in Non-ductile Reinforced Concrete Frames Using Engineered Cementitious Composites Stanford University; 2011.
[7] Altin S, Anil Ö, Kara ME. Strengthening of RC nonductile frames with RC infills: An experimental study. Cement and Concrete Composites. 2008;30:612-21.
[8] Mosalam K, White R, Gergely P. Static Response of Infilled Frames Using Quasi-Static Experimentation. Journal of Structural Engineering. 1997;123:1462-4169.
[9] DolŠEk M, Fajfar P. Soft Storey Effects in Uniformly Infilled Reinforced Concrete Frames. Journal of Earthquake Engineering. 2001;5:1-12.
[10] Yuksel E, Ozkaynak H, Buyukozturk O, Yalcin C, Dindar AA, Surmeli M, et al. Performance of alternative CFRP retrofitting schemes used in infilled RC frames. Construction and Building Materials. 2010;24:596-609.

[11] Crisafulli F. Seismic Behavior of Reinforced Concrete Structures with Masonry Infills. New Zealand: University of Canterbury; 1997.

[12] Kakaletsis DJ, Karayannis CG. Influence of Masonry Strength and Openings on Infilled R/C Frames Under Cycling Loading. Journal of Earthquake Engineering. 2008;12:197-221.

[13] Surendran S, Kaushik HB. Masonry infill RC frames with openings: review of in-plane lateral load behaviour and modeling approaches. The Open Construction and Building Technology Journal. 2012;6:126-54.

[14] Liauw TC, Kwan KH. Static and cyclic behaviours of multistorey infilled frames with different interface conditions. Journal of Sound and Vibration. 1985;99:275-83.

[15] Mallick DV, Severn RT. The Behaviour of Infilled Frames Under Static Loading. ICE Proceedings1967. p. 639-56.

[16] Cavaleri L, Papia M. A new dynamic identification technique: application to the evaluation of the equivalent strut for infilled frames. Engineering Structures. 2003;25:889-901.

[17] Holmes M. Steel Frames with Brickwork and Concrete Infilling. ICE Proceedings1961. p. 473-8.

[18] Crisafulli FJ, Carr AJ. Proposed macro-model for the analysis of infilled frame structures. Bulletin of the New Zealand society for earthquake engineering. 2007;40.

[19] Smyrou E, Blandon C, Antoniou S, Pinho R, Crisafulli F. Implementation and verification of a masonry panel model for nonlinear dynamic analysis of infilled RC frames. Bull Earthquake Eng. 2011;9:1519-34.

[20] Lourenço PB. Computational strategies for masonry structures [Diss , Technische Universiteit Delft, 1996]. Delft: Delft University Press; 1996.